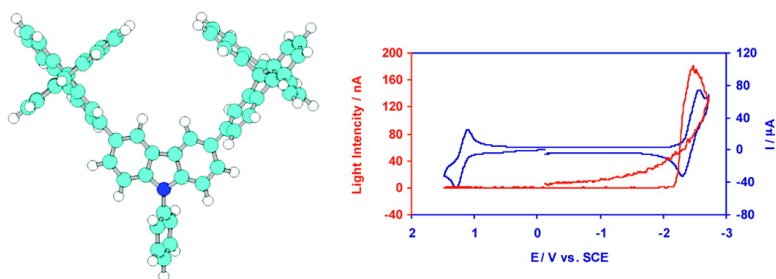


## Electrochemistry and Electrogenerated Chemiluminescence of 3,6-Di(spirobifluorene)-*N*-phenylcarbazole

Sahar Rashidnadi, Tsung Hsi Hung, Ken-Tsung Wong, and Allen J. Bard

*J. Am. Chem. Soc.*, **2008**, 130 (2), 634-639 • DOI: 10.1021/ja076033x

Downloaded from <http://pubs.acs.org> on February 8, 2009



### More About This Article

Additional resources and features associated with this article are available within the HTML version:

- Supporting Information
- Links to the 1 articles that cite this article, as of the time of this article download
- Access to high resolution figures
- Links to articles and content related to this article
- Copyright permission to reproduce figures and/or text from this article

[View the Full Text HTML](#)



## Electrochemistry and Electrogenerated Chemiluminescence of 3,6-Di(spirobifluorene)-*N*-phenylcarbazole

Sahar Rashidnadimi, Tsung Hsi Hung, Ken-Tsung Wong, and Allen J. Bard\*

*Department of Chemistry and Biochemistry, The University of Texas at Austin, Austin, Texas 78712, and Department of Chemistry, National Taiwan University, 106 Taipei, Taiwan*

Received August 10, 2007; E-mail: ajbard@mail.utexas.edu

**Abstract:** We report here the electrochemistry, luminescence, and electrogenerated chemiluminescence (ECL) of 3,6-dispirobifluorene-*N*-phenylcarbazole (DSBFNPC). DSBFNPC contains two spirobifluorene groups covalently attached to the *N*-phenylcarbazole core. The optimized geometry as determined from semiempirical MNDO calculations shows that the phenyl group is twisted 89° from the plane of central carbazole, indicating a lack of electron delocalization between these groups. However, the two fluorene rings of each spirobifluorene group are twisted 58° relative to each other and two spirobifluorene groups are twisted 64° from the *N*-phenylcarbazole ring, suggesting some charge delocalization among these groups. The cyclic voltammetry of this compound shows two reversible oxidation waves (assigned to the formation of the cation and dication) and a two-electron reduction wave that becomes reversible at higher scan rates (assigned to formation of anion). Digital simulations were carried out to obtain details of the electrochemical processes, and electrochemical behavior was compared to that of phenylcarbazole (PC). Upon cycling between the oxidation and reduction waves, ECL is produced by radical ion annihilation. The photophysical properties of DSBFNPC show a strong resemblance to the parent compound, PC, and the ECL spectrum produced via radical ion annihilation shows good agreement with the fluorescence emission spectrum of DSBFNPC.

### Introduction

We describe here the electrochemical reduction, oxidation, and radical ion annihilation electrogenerated chemiluminescence (ECL) of a new spirobifluorene (SBF) compound modified with an *N*-phenylcarbazole (NPC) bridge (3,6-dispirobifluorene-*N*-phenylcarbazole, DSBFNPC). The fluorene moiety absorbs strongly in the UV region, fluoresces in the visible region, and shows good chemical and photochemical stability. Fluorene-based macromolecules such as terfluorenes,<sup>1,2</sup> oligomeric fluorenes,<sup>2,3</sup> and polyfluorenes<sup>4,5</sup> are of interest in organic light-emitting devices (OLED) because of their efficient blue-light emitting characteristics and good chemical and thermal stabilities. Fluorene polymers have been extensively studied as electron transport materials<sup>6</sup> and have also found applications as nonlinear optic materials<sup>7,8</sup> and in photovoltaic cells.<sup>9,10</sup> Ter-

(9,9-diarylfuorene)s<sup>1</sup> show good optical and electrochemical properties, such as high fluorescence quantum yields in solution as well as in thin films of interest in OLEDs. They also show high mobility of both electrons and holes in amorphous films,<sup>11</sup> and they are, therefore, good candidates for blue-light emitters in ECL.<sup>12</sup> We have previously reported the electrochemical behavior and ECL of ter(9,9-diarylfuorene)s<sup>12</sup> and spirobifluorene-bridged bipolar systems<sup>13</sup> with stable radical ions. This work describes the electrochemical reduction, oxidation, and radical ion annihilation electrogenerated chemiluminescence (ECL) of a new spirobifluorene compound modified with an *N*-phenylcarbazole bridge (DSBFNPCB).

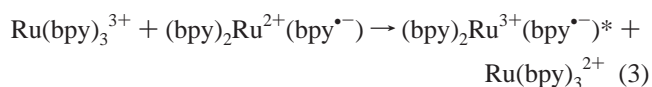
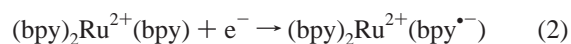
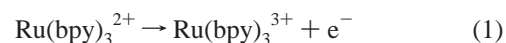
In ECL, an excited state is produced by an energetic electron-transfer reaction between electrochemically generated species, often radical ions.<sup>14</sup> This ion annihilation reaction occurs in the diffusion layer near the electrode and is accomplished by

- (1) Wong, K.-T.; Chien, Y.-Y.; Chen, R.-T.; Wang, C.-F.; Lin, Y.-T.; Chiang, H.-H.; Hsieh, P.-Y.; Wu, C.-C.; Chou, C. H.; Su, Y. O.; Lee, G.-H.; Peng, S.-M. *J. Am. Chem. Soc.* **2002**, *124*, 11576.
- (2) Geng, Y.; Katsis, D.; Culligan, S. W.; Ou, J. J.; Chen, S. H.; Rothberg, L. *J. Chem. Mater.* **2002**, *14*, 463.
- (3) Katsis, D.; Geng, Y. H.; Ou, J. J.; Culligan, S. W.; Trajkovska, A.; Chen, S. H.; Rothberg, L. *J. Chem. Mater.* **2002**, *14*, 1332.
- (4) Chang, S.-C.; Li, Y.; Yang, Y. *J. Phys. Chem. B* **2000**, *104*, 11650.
- (5) Lupton, J. M.; Craig, M. R.; Meijer, E. W. *Appl. Phys. Lett.* **2002**, *80*, 4489.
- (6) Mueller, C. D.; Falcou, A.; Reckefuss, N.; Rojahn, M.; Wiederhirn, V.; Rudati, P.; Frohne, H.; Nuyken, O.; Becker, H.; Meerholz, K. *Nature* **2003**, *421*, 829.
- (7) Epshtein, O.; Eichen, Y.; Ehrenfreund, E.; Wohlgenannt, M.; Vardeny, Z. *V. Phys. Rev. Lett.* **2003**, *90*, 046804/1.
- (8) Zhan, X.; Liu, Y.; Zhu, D.; Liu, X.; Xu, G.; Ye, P. *Chem. Phys. Lett.* **2002**, *362*, 165.
- (9) Cabanillas-Gonzalez, J.; Yeates, S.; Bradley, D. D. C. *Synth. Met.* **2003**, *139*, 637.
- (10) Pacios, R.; Bradley, D. D. C. *Synth. Met.* **2002**, *127*, 261.
- (11) Wu, C.-C.; Liu, T.-L.; Hung, W.-Y.; Lin, Y.-T.; Wong, K.-T.; Chen, R.-T.; Chen, Y.-M.; Chien, Y.-Y. *J. Am. Chem. Soc.* **2003**, *125*, 3710.
- (12) Choi, J. P.; Wong, K. T.; Chen, Y. M.; Yu, J. K.; Chou, P. T.; Bard, A. J. *J. Phys. Chem. B* **2003**, *107*, 14407.
- (13) Fungo, F.; Wong, K.-T.; Ku, S.-Y.; Hung, Y.-Y.; Bard, A. J. *J. Phys. Chem. B* **2005**, *109*, 3984.
- (14) (a) Faulkner, L. R.; Bard, A. J. *Electroanalytical Chemistry*; Marcel Dekker: New York, 1977; Vol. 10, p 1. (b) Bard, A. J.; Debad, J. D.; Leland, J. K.; Sigal, G. B.; Wilbur, J. L.; Wohlstadter, J. N. *Encyclopedia of Analytical Chemistry: Applications, Theory, and Instrumentation*; Meyers, R. A., Ed.; Wiley & Sons: New York, 2000; Vol. 11, p 9842 and references therein. (c) *Electrogenerated Chemiluminescence*; Bard, A. J., Ed.; Marcel Dekker: New York, 2004.

alternating pulsing or sweeping the potential to produce the reactants. The electron-transfer reaction (ion annihilation) can produce excited singlet or triplet states, depending on the energy of the reaction and the energy of the excited state. If the magnitude of the enthalpy ( $\Delta H_{\text{ann}}$ ) of an ion annihilation reaction is larger than the energy ( $E_s$ ) needed for the excited singlet state, the direct generation of an excited singlet state is possible; this is called the S-route or an energy-sufficient system.<sup>14</sup> If  $|\Delta H_{\text{ann}}|$  of the ion annihilation reaction is lower than  $E_s$  but higher than the triplet state energy ( $E_t$ ), the generation of an excited singlet state is still possible by a triplet–triplet annihilation reaction (a T-route or energy-deficient system).<sup>14</sup> If  $|\Delta H_{\text{ann}}|$  is close to  $E_s$ , the T-route can contribute to the formation of singlet state species in addition to the S-route, and this is called the ST-route.<sup>15,16</sup> In some cases, excimer or exciplex emission has also been observed (the E-route).<sup>14</sup> Many polyaromatic hydrocarbons, the first compounds studied for ECL applications, produced emission by these reaction schemes.<sup>14,17</sup>

Useful ECL compounds must be able to generate stable radical cations and anions with sufficient energy in the electron-transfer reaction to generate an excited state that emits with good quantum efficiency. However, many molecules that emit strongly do not produce strong ECL, because decomposition of the radical ion causes one of the redox processes to be chemically irreversible. In others, the radical cation or anion cannot be generated before the background oxidation or reduction of the solvent-supporting electrolyte. In these cases, ECL coreactants can be added to generate a stable radical counterion required for annihilation.<sup>14</sup> ECL coreactants are species that, upon electrochemical oxidation or reduction, undergo a bond cleavage reaction to produce intermediates that are strong reductants or oxidants, capable of reacting with one of the electrogenerated species to produce excited states capable of emitting light.<sup>18</sup>

In recent years, compounds that contain a coreactant directly attached to the emitting dye with one reversible electrochemical process, or compounds that have donor and acceptor moieties covalently bonded with a capability to generate ECL through charge-transfer states, have been studied<sup>19,20</sup> with the hope of improving the radical cation and anion stability and obtaining structures that contain charge-transfer characteristics analogous to those of  $\text{Ru}(\text{bpy})_3^{2+}$ . In this case, the oxidized form is a Ru(III) center and the reduced form is a bipyridine radical anion. The excited state can be written as the well-known charge-transfer state shown in the following reactions



In this case, the oxidized form contains a Ru(III) center and the reduced form contains a bipyridine radical anion. The excited state can be written as the charge-transfer state shown in eqs 3 and 4. The fluorene ring provides a good emitting center but has poor cation radical stability so it is not a good candidate for ECL. However, by functionalization with the appropriate redox center, it is possible to improve the stability of the oxidized fluorene compound for ECL. As discussed earlier, because of their attractive properties, 9,9'-spirobifluorene derivatives have been proposed as suitable materials in the field of photoelectronic devices, including ECL devices and photovoltaic cells.<sup>12,13,21</sup> Molecules incorporating carbazole moieties have been investigated extensively as light-emitting materials and as hole-transporting materials in OLEDs because of their high reversibility upon electrochemical oxidation.<sup>22</sup> For example, poly(*N*-vinyl carbazole) is often used as a hole transport layer,<sup>23</sup> and highly efficient devices with this polymer as a hole transport polymer have been reported.<sup>24</sup> Recently, luminescent thin films of conjugated polymers containing both of the fluorene and carbazole moieties as the emitting layer for OLEDs have been reported.<sup>25,26</sup> The fluorene moieties with strong blue fluorescence play the key role of luminescing sites, and the carbazole units with coupling activity under anodic oxidation play the role of the linking sites in electropolymerization. In addition, a non-conjugated hybrid of carbazole and fluorene has been reported to produce efficient green and red electrophosphorescent devices.<sup>27</sup> This new material combines characteristics of both carbazole and fluorene.

## Experimental Section

**Materials.** *N*-Phenylcarbazole (Aldrich) and anhydrous acetonitrile (MeCN, Aldrich) were used without further purification, and anhydrous benzene (Aldrich) was used after distillation. Tetra-*n*-butylammonium hexafluorophosphate (TBAPF<sub>6</sub>) (Aldrich) was dried in a vacuum oven at 125 °C before being transferred directly into an inert atmosphere glovebox (Vacuum Atmospheres Corp.). All solutions were prepared in the glovebox with fresh anhydrous solvents and sealed in airtight vessels for measurements completed outside the box.

**Synthesis.** A mixture of 3,6-dipicolonic ester-9-phenylcarbazole<sup>36</sup> (495 mg, 1.0 mmol), 2-bromo-9,9'-spirobifluorene<sup>1</sup> (827 mg, 2.1 mmol), Pd(PPh<sub>3</sub>)<sub>4</sub> (213 mg, 0.2 mmol), P(*t*-Bu)<sub>3</sub> (2 mL, 0.05 M in

(15) Bezman, R.; Faulkner, L. R. *J. Am. Chem. Soc.* **1972**, *94*, 6317.

(16) Tachikawa, H.; Bard, A. J. *Chem. Phys. Lett.* **1974**, *26*, 246.

(17) (a) Knight, A. W.; Greenway, G. M. *Analyst* **1994**, *119*, 879. (b) Maloy, J. T.; Bard, A. J. *J. Am. Chem. Soc.* **1971**, *93*, 5968. (c) Bezman, R.; Faulkner, L. R. *J. Am. Chem. Soc.* **1972**, *94*, 6324. (d) Debad, J. D.; Morris, J. C.; Lynch, V.; Magnus, P.; Bard, A. J. *J. Am. Chem. Soc.* **1996**, *118*, 2374. (e) Debad, J. D.; Morris, J. C.; Magnus, P.; Bard, A. J. *J. Org. Chem.* **1997**, *62*, 530.

(18) (a) Chang, M.-M.; Saji, T.; Bard, A. J. *J. Am. Chem. Soc.* **1977**, *99*, 5399. (b) Rubinstein, I.; Bard, A. J. *J. Am. Chem. Soc.* **1981**, *103*, 512. (c) White, H. S.; Bard, A. J. *J. Am. Chem. Soc.* **1982**, *104*, 6891.

(19) (a) Kapturkiewicz, A.; Grabowski, Z.; Jasny, J. *J. Electroanal. Chem.* **1990**, *279*, 55. (b) Kapturkiewicz, A. *Chem. Phys.* **1992**, *166*, 259. (c) Kapturkiewicz, A.; Herbich, J.; Nowacki, J. *Chem. Phys. Lett.* **1997**, *275*, 355.

(20) (a) Lai, R. Y.; Kong, X.; Jenekhe, S. A.; Bard, A. J. *J. Am. Chem. Soc.* **2003**, *125*, 12631. (b) Lai, R. Y.; Fabrizio, E. F.; Lu, L.; Jenekhe, S. A.; Bard, A. J. *J. Am. Chem. Soc.* **2001**, *123*, 9112.

(21) (a) Wong, K.-T.; Liao, Y.-L.; Lin, Y.-T.; Su, H.-C.; Wu, C.-C. *Org. Lett.* **2005**, *7*, 5131. (b) Bach, U.; Lupo, D.; Comte, P.; Moser, J. E.; Weissortel, F.; Salbeck, J.; Spreitzer, H.; Gratzel, M. *Nature* **1998**, *395*, 583.

(22) (a) Kundu, P.; Justin Thomas, K. R.; Lin, J. T.; Tao, Y.-T.; Chien, C.-H. *Adv. Funct. Mater.* **2003**, *13*, 445. (b) Wong, K.-T.; Hung, T.-H.; Chao, T.-C.; Ho, T.-I. *Tetrahedron Lett.* **2005**, *46*, 855.

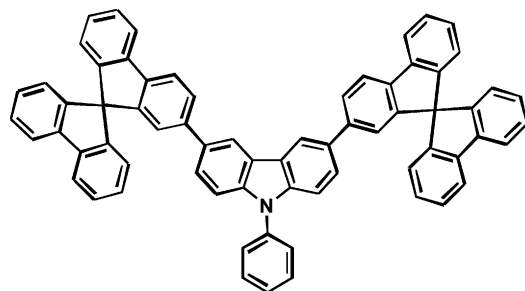
(23) Kido, J.; Hongawa, K.; Okuyama, K.; Nagai, K. *Appl. Phys. Lett.* **1993**, *63*, 2627.

(24) Zhu, W. H.; Hu, C.; Chen, K. C.; Tian, H. *Synth. Met.* **1998**, *96*, 151.

(25) Xie, C.; Advincula, R. C.; Baba, A.; Knoll, W. *Chem. Mater.* **2004**, *16*, 2852.

(26) Li, M.; Tang, S.; Shen, F.; Liu, M.; Xie, W.; Xia, H.; Liu, L.; Tian, L.; Xie, Z.; Lu, P.; Hanif, M.; Lu, D.; Cheng, G.; Ma, Y. *J. Phys. Chem. B* **2006**, *110*, 17784.

(27) Wong, K.-T.; Chen, Y.-M.; Lin, Y.-T.; Su, H.-C.; Wu, C.-C. *Org. Lett.* **2005**, *7*, 5361.



DSBFNPC

toluene, 0.1 mmol), and  $\text{Na}_2\text{CO}_3$  (3 mL, 2 M) in toluene (30 mL) was refluxed for 3 days. The reaction mixture was extracted with  $\text{CH}_2\text{Cl}_2$ , and the combined organic solution was dried over  $\text{MgSO}_4$  and concentrated. The desired product (DSBFNPC) was isolated by column chromatography on silica gel ( $\text{CHCl}_3/n\text{-hexanes} = 1/4$ ) as a solid (548 mg, 63%). Mp 410 °C (DSC); IR (KBr)  $\nu$  731, 1268, 1447, 1500, 1600, 3032  $\text{cm}^{-1}$ ;  $^1\text{H}$  NMR (400 MHz,  $\text{CDCl}_3$ )  $\delta$  6.75 (d,  $J = 7.6$  Hz, 2H), 6.83 (d,  $J = 7.6$  Hz, 4H), 7.05 (s, 2H), 7.12–7.17 (m, 6H), 7.29 (d,  $J = 8.4$  Hz, 2H), 7.38–7.43 (m, 7 H), 7.47 (t,  $J = 6.4$  Hz, 4H), 7.56 (t,  $J = 7.6$  Hz, 2H), 7.73 (dd,  $J = 2.0, 8.0$  Hz, 2 H), 7.89 (d,  $J = 7.6$  Hz), 7.94 (d,  $J = 8.0$  Hz, 2 H), 8.16 (s, 2H);  $^{13}\text{C}$  NMR (100 MHz,  $\text{CDCl}_3$ )  $\delta$  66.0, 109.8, 118.8, 119.9, 120.0, 120.2, 122.8, 123.7, 123.9, 124.2, 125.6, 126.8, 127.0, 127.4, 127.6, 127.7, 127.8, 129.8, 133.3, 137.4, 140.3, 140.5, 141.5, 141.6, 141.8, 148.8, 149.1, 149.3; MS ( $m/z$ , FAB) 872.4; HRMS ( $\text{M}^+$ , FAB) Calcd for  $\text{C}_{68}\text{H}_{41}\text{N}$ , 871.3239; found, 871.3238; Anal. Calcd for  $\text{C}_{68}\text{H}_{41}\text{N}$ : C, 93.65; H, 4.74; N, 1.61. Found: C, 93.80; H, 4.39; N, 1.54.

**Characterization.** Absorption spectra were obtained with a Milton Roy Spectronic 3000 array spectrophotometer, and the steady-state fluorescence spectra were recorded at room temperature using a PTI spectrofluorimeter (model QM-2000; PhotonTechnology International). The absorbance spectrum of DSBFNPC was obtained with a 6  $\mu\text{M}$  solution prepared with 1:1 benzene/acetonitrile (PhH/MeCN), and the fluorescence spectrum of the same compound was obtained with a 0.5  $\mu\text{M}$  solution in 1:1 PhH/MeCN. The relative fluorescence efficiency was measured using a 0.5  $\mu\text{M}$  solution in PhH/MeCN (1:1) and calibrated with diphenylanthracene (DPA) as a standard ( $\lambda_{\text{exc}} = 380$  nm;  $\phi_{\text{DPA}} = 0.91$  in benzene).<sup>28</sup>

Cyclic voltammograms were recorded on an electrochemical workstation (CH Instruments). The working electrode in all cases consisted of an inlaid platinum disk (2.0-mm diameter) that was polished on a felt pad with 0.3- $\mu\text{m}$  alumina (Buehler, Ltd.), sonicated in water and absolute ethanol for 10 min, and then dried in an oven at 100 °C before being transferred into the glovebox. A platinum coil served as a counter electrode, and a silver wire was utilized as a quasi-reference electrode (QRE). The concentrations and solvents used to obtain each voltammogram are given in the corresponding figure caption. All potentials were calibrated versus an aqueous SCE by the addition of ferrocene as an internal standard taking  $E_{(\text{Fc}/\text{Fc}^+)}^0 = 0.424$  V vs SCE.<sup>29</sup> Digital simulations were performed using DigiElch version 2.0.<sup>30</sup> All electron-transfer reactions were considered fast ( $k^0 = 10$  cm  $\text{s}^{-1}$ ); all  $\alpha$  values were taken to be 0.5. Other parameters used for the digital simulations are given in the figure caption. MNDO semiempirical calculations were performed with HyperChem by Hypercube, Inc.

ECL measurements were performed as previously reported.<sup>31</sup> To generate the annihilation reaction, the working electrode was pulsed

- (28) Stevens, B.; Algar, B. J. *Phys. Chem.* **1968**, *72*, 2582.  
 (29) Debad, J. D.; Morris, J. C.; Magnus, P.; Bard, A. J. *J. Org. Chem.* **1997**, *62*, 530.  
 (30) (a) Rudolph, M. J. *Electroanal. Chem.* **2003**, *543*, 23. (b) Ruldolf, M. J. *Electroanal. Chem.* **2004**, *571*, 289. (c) Rudolph, M. J. *Electroanal. Chem.* **2003**, *558*, 171. (d) Rudolph, M. J. *Comput. Chem.* **2005**, *26*, 619. (e) Rudolph, M. J. *Comput. Chem.* **2005**, *26*, 633. (f) Rudolph, M. J. *Comput. Chem.* **2005**, *26*, 1193.  
 (31) McCord, P.; Bard, A. J. *J. Electroanal. Chem. Interfacial Electrochem.* **1991**, *318*, 91.

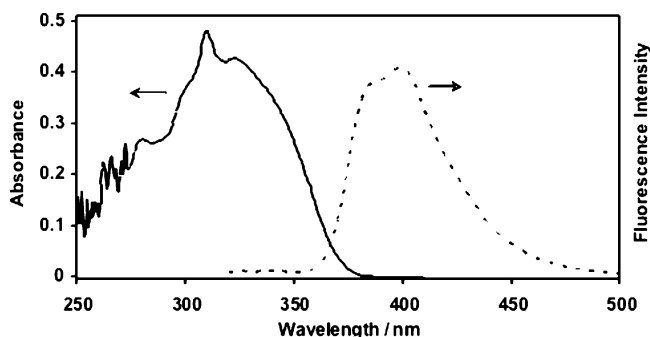
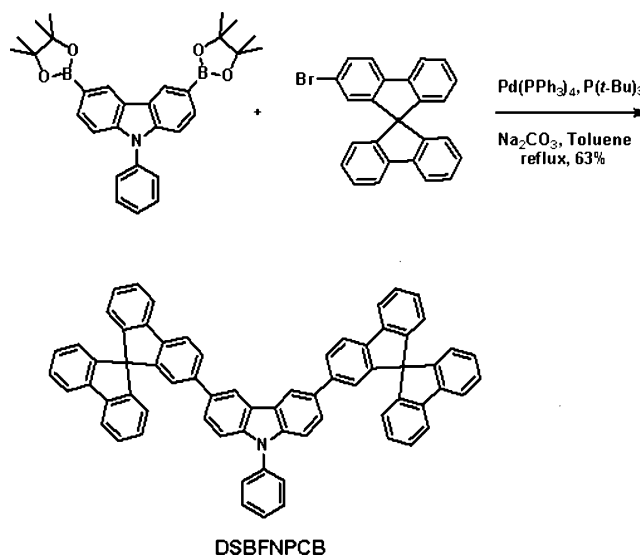


**Figure 1.** Absorbance spectra (5.7  $\mu\text{M}$ ) (solid line) and fluorescence spectra (0.53  $\mu\text{M}$ ) (dotted line) of solution of DSBFNPC in 1:1 PhH/MeCN (excitation wavelength, 310 nm).

### Scheme 1 Synthesis of DSBFNPCB



between the first oxidation and reduction peak potentials of the 3,6-dispirofluorene-*N*-phenylcarbazole with a pulse width of 0.02 s. The resulting emission spectra were obtained with a charged coupled device (CCD) camera (Photometrics CH260, Photometrics-Roper Scientific) that was cooled to  $-100$  °C. Integration times were 1 min. The CCD camera and grating system were calibrated with a mercury lamp before each measurement.

## Results and Discussion

**Synthesis.** The titled compound was synthesized in moderate yield of 63% by coupling the 2-bromo-9,9'-spirobifluorene with 3,6-diphenylboronic ester-9-phenylcarbazole in the presence of a catalytic amount of  $\text{Pd}(\text{PPh}_3)_4$  and cocatalyst  $\text{P}(t\text{-Bu})_3$  in toluene (Scheme 1).

**Absorption and Emission Spectroscopy.** Absorption and fluorescence spectra of DSBFNPC are shown in Figure 1. The absorption spectrum that was obtained in the same solvent mixture used for all electrochemical measurements shows a very broad band ranging from 275 to 365 nm with a  $\lambda_{\text{max}}$  at 310 nm and three shoulders at  $\lambda_1 = 278$  nm,  $\lambda_2 = 300$  nm, and  $\lambda_3 = 323$  nm. The plot of absorbance vs concentration shows a high molar absorptivity ( $\epsilon = 79\,560$   $\text{cm}^{-1}$   $\text{M}^{-1}$ ) (Supporting Information). This solution emitted in the blue region when excited at 310 nm (a shoulder around 385 nm and  $\lambda_{\text{max}} = 400$  nm) with a moderately high fluorescence efficiency,  $\phi = 0.65$ . In addition to the broad absorption, a relatively large Stokes shift of 70 nm was observed between the absorption and emission spectral

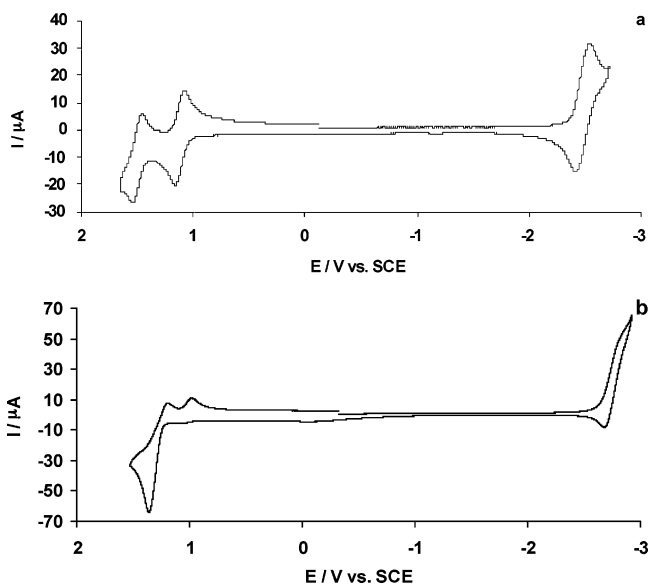


**Figure 2.** (a) Cyclic voltammogram of a 1 mM solution of DSBFNPC in 0.1 TBAPF<sub>6</sub> in 1:1 PhH/MeCN at a platinum electrode (area = 0.031 cm<sup>2</sup>) (scan rate, 1 V/s). (b) Cyclic voltammogram of a 1 mM solution of NPC in 0.1 TBAPF<sub>6</sub> in 1:1 PhH/MeCN at a platinum electrode (area = 0.031 cm<sup>2</sup>) (scan rate, 1 V/s).

maxima. Phenylcarbazole showed about the same absorption maximum ( $\lambda_{\text{max}} = 339$  nm in MeCN), but its fluorescence emission is at  $\lambda_{\text{max}} = 339$ ,<sup>32</sup> so that the fluorescence spectra of DSBFNPC ( $\lambda_{\text{max}} = 400$  nm) is red shifted by 61 nm when compared to that of PC because of the more conjugated structure. On the basis of the emission wavelengths in the fluorescence spectrum, the energy needed to generate the first singlet excited state is about 3.1 eV; therefore, it is this energy that must be generated in the electrochemical annihilation reaction of the radical ions to produce the singlet excited state and ECL emission.

**Electrochemical Properties of DSBFNPC.** A cyclic voltammogram of DSBFNPC in 0.1 M TBAPF<sub>6</sub> in PhH/MeCN obtained at a platinum electrode is shown in Figure 2a. Upon scanning the potential positive, two reversible one-electron oxidation waves were observed: first wave at half-wave potential,  $E_{1/2}$ , of +1.12 V vs SCE and second wave at +1.50 V vs SCE. These waves correspond to the formation of the radical cation ( $i_{\text{pa}1} = -18.1 \mu\text{A}$ ) and the dication ( $i_{\text{pa}2} = -15.4 \mu\text{A}$ ). The observed peak separation for the reversible waves was  $\sim 85$  mV, larger than that expected for a Nernstian one-electron wave (59 mV). However, the internal standard, ferrocene, which is known to show Nernstian behavior, showed a similar peak separation under these same electrolyte conditions; thus, the observed peak separation can be attributed to ohmic drop ( $\sim 750 \Omega$ ) that is often observed with this aprotic solvent. Scan rate studies (Supporting Information) showed that the anodic and cathodic peak currents ( $i_{\text{pa}}$ ,  $i_{\text{pc}}$ ) of the both oxidation waves were proportional to the square root of scan rate ( $\nu^{1/2}$ ). Additionally, the peak current ratio ( $i_{\text{pa}}/i_{\text{pc}}$ ) was approximately unity down to a scan rate of 50 mV/s, indicating the absence of a following chemical reaction and good stability of the radical cation and dication.

Upon scanning in the negative direction, one reduction wave with an  $E_{1/2}$  of  $-2.49$  V vs SCE was observed. Direct

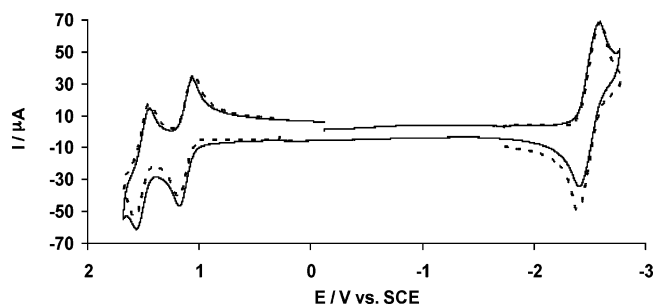


**Figure 3.** Cyclic voltammogram of a 1 mM solution of DSBFNPC in 0.1 M TBAPF<sub>6</sub> in 1:1 PhH/MeCN at a platinum electrode (area = 0.031 cm<sup>2</sup>) (scan rate = 5 V/s) (solid line). The dotted line shows a simulated voltammogram of DSBFNPC at a scan rate of 5 V/s. Parameters:  $R = \text{DSBFNPC}$ ,  $E_{\text{RR}^{+\circ}}^0 = 1.12$  V,  $E_{\text{RR}^{2+}}^0 = 1.51$  V,  $E_{\text{RR}^{-\circ}}^0 = -2.45$  V,  $E_{\text{RR}^{2-}}^0 = -2.51$  V (vs SCE),  $C_{\text{R}} = 1$  mM,  $R_{\text{u}} = 750 \Omega$ ,  $C_{\text{d}} = 0.7 \mu\text{F}$ ,  $T = 298$  °C, planar electrode area = 0.031 cm<sup>2</sup>,  $D = 4.3 \times 10^{-6}$  cm<sup>2</sup>/s,  $k^{\circ} = 10$  cm/s, and  $\alpha = 0.5$  for all heterogeneous electron-transfer reactions.

comparison to the one-electron oxidation waves indicates that this reduction wave appears to be a single two-electron wave ( $i_{\text{pc}} = 30.0 \mu\text{A}$ ). This wave, therefore, corresponds to the formation of the dianion. This wave is not completely reversible at low scan rate (Supporting Information) presumably because the dianion is basic enough to abstract protons from any proton donor present in the medium (e.g., trace water). This following reaction makes the reduction wave irreversible ( $i_{\text{pc}} \gg i_{\text{pa}}$ ) at low scan rates (e.g., 50 mV/s), but at high scan rates ( $\nu > 1$  V/s) good reversibility was observed and  $i_{\text{pa}}/i_{\text{pc}}$  was close to unity at  $\nu = 5$  V/s. Additionally, at a more negative potential, another two-electron wave appears that corresponds to the formation of a tetraanion (Supporting Information). The first reduction showed  $i_{\text{pc}}$  proportional to  $\nu^{1/2}$ , indicating diffusion control of the electrode reaction. However,  $E_{\text{pa}}$  and  $E_{\text{pc}}$  shifted with scan rate because of the uncompensated resistance.

It is instructive to compare the behavior of DSBFNPC to that of *N*-phenylcarbazole under the same electrochemical conditions.<sup>33,34</sup> A cyclic voltammogram is shown in Figure 2b. The oxidation of NPC showed a much less reversible behavior at 1 V/s at a slightly more positive potential than DSBFNPC ( $E_{1/2} = 1.30$  V vs SCE), which has been attributed to the formation of an unstable radical cation that undergoes a dimerization reaction.<sup>33,34</sup> The electrochemical reduction behavior of NPC shows a less reversible wave at a significantly more negative potential ( $E_{1/2} = -2.755$  V vs SCE).

To confirm the proposed electrochemical reaction scheme of DSBFNPC in this solvent-electrolyte system, digital simulations of the cyclic voltammetry were carried out. Figure 3 shows two simulated cyclic voltammograms (dotted line) in a 1 mM solution of DSBFNPC at a scan rate of 5 V/s, with the parameters shown in the figure caption. The good fit between the experimental and theoretical voltammograms supports the assumption that the oxidation waves obtained experimentally are two spaced consecutive one-electron oxidations, and the reduction wave involves an overall two-electron reduction at essentially the same reduction potential or, more exactly, two one-electron reductions with a potential difference of less than 60 mV between the  $E^{\circ}$  values. Similar results were obtained at other scan rates with the same parameters (Supporting Information).

(32) Kadiri, A.; Benali, B.; Boucetta, A.; Kabouchi, B. *Spectrochim. Acta* **1993**, *49A*, 1547.

(33) Ambrose, J. F.; Carpenter, L. L.; Nelson, R. F. *J. Electrochem. Soc.* **1975**, *122*, 876.

(34) Oyama, M.; Matsui, J. *Bull. Chem. Soc. Jpn.* **2004**, *77*, 953.

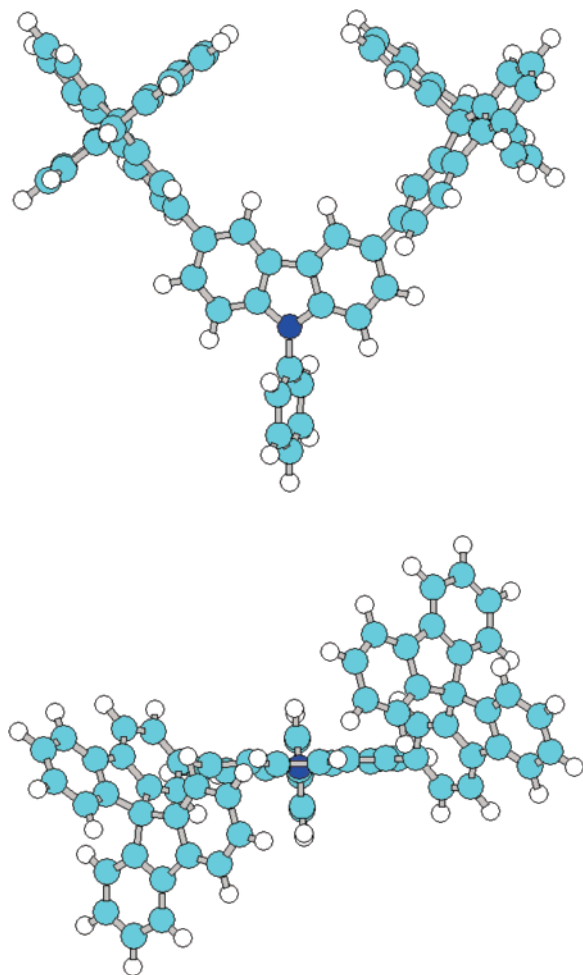


**Figure 4.** Two views of DSBFNPC with optimized ground-state molecular geometry as calculated by MNDO semiempirical calculations.

MNDO semiempirical calculations were used to obtain optimized molecular geometry of this compound to gauge the extent of charge localization upon the oxidation and reduction of DSBFNPC. As shown in Figure 4, the phenyl group is twisted  $89^\circ$  from the plane of central carbazole, indicating a lack of electron delocalization among these groups. Moreover, two fluorene rings of each spirobifluorene groups are twisted  $58^\circ$  relative to each other, and two spirobifluorene groups are twisted  $64^\circ$  from the plane of the *N*-phenylcarbazole ring, suggesting only a small amount of charge delocalization between these two groups. This is consistent with the electrochemical behavior of DSBFNPC in which the oxidation is primarily in the NPC part and results in the two separated one-electron oxidation waves of the NPC moiety. The fact that the potential of oxidation of DSBFNPC is slightly less positive than that for NPC suggests a small amount of delocalization to both spirobifluorene groups. However, the calculated structure suggests only a small amount of delocalization between the two spirobifluorene groups and so that each accepts an electron independently (except for a small statistical factor<sup>35</sup>), resulting in the two-electron reduction wave of DSBFNPC, essentially involving the formation of a radical anion for each of the spirobifluorene groups. The second

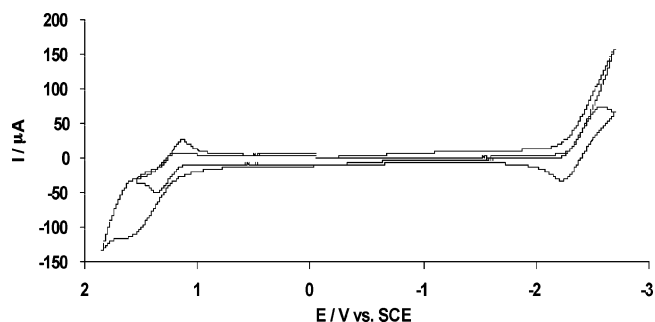


**Figure 5.** Cyclic voltammograms of a 1 mM solution of DSBFNPC in 1:12 PhH/MeCN at a platinum electrode before and after applying 500 potential pulses between +1.42 and  $-2.63$  V (vs SCE) (0.1 M TBAPF<sub>6</sub>; scan rate = 5 V/s).

two-electron reduction is similarly the formation of the dianion on each group.

Upon continuous potential cycling of a solution of DSBFNPC over the range that encompassed the first oxidation and first reduction waves, the first two-electron reduction wave became irreversible, and the loss of reversibility became more pronounced as the number of scans increased. Figure 5 shows cyclic voltammograms that were obtained before and after applying numerous potential pulses with the pulsing potential set at 50 mV past the peak potentials of the first oxidation and reduction waves of DSBFNPC ( $+1.42$  and  $-2.63$  V vs SCE). The loss of reversibility indicates a slow following chemical reaction involving the oxidized and reduced species. Since this behavior is only observed upon scanning over both the oxidation and reduction waves (i.e., it is not found when cycling only over the first oxidation or only over the first reduction waves), the reaction also appears to involve the radical cation of *N*-phenylcarbazole moiety.<sup>33,34</sup> The products of this reaction form an insoluble film on the surface of the platinum working electrode, which alters the electrochemical behavior of both DSBFNPC in solution as well as the internal potential standard, ferrocene (voltammogram not shown).

As a final note, the total free energy of the annihilation reaction ( $\Delta G_{\text{anni}} = \Delta H_s - T\Delta S$ ), which is based on the difference between the peak potentials of the first oxidation and first reduction wave in the cyclic voltammogram ( $\Delta E_{\text{p(ox/red)}} = 3.6$  eV) with entropy effects ( $\sim 0.1$  eV) subtracted out, is about 3.5 eV.<sup>14</sup> This energy, which becomes available upon radical ion annihilation, is greater than that required to directly populate the singlet excited state (3.1 eV) as previously determined from the fluorescence spectrum. This large difference in potentials suggests that the electron transfers involve fairly isolated units while the luminescence involves a charge-transfer transition, as discussed earlier for another spirobifluorene system.<sup>13</sup>

**Electrogenerated Chemiluminescence.** Figure 6 shows the ECL spectrum of DSBFNPC in PhH/MeCN (1:1) containing 0.1 M TBAPF<sub>6</sub> as supporting electrolyte during repeated pulsing (pulse width = 0.02 s) between potentials where oxidized and reduced forms are alternately produced. The instability of the radical ions as well as the film may pose problems in obtaining ECL over a long time period; however, by trying many short pulse widths, we were able to observe ECL. In a typical ECL experiment, the radical anion reacts with the radical cation; however, in our case, we are generating the dianion or, more appropriately, the radical anion of each spirobifluorene group

(35) Bard, A. J.; Faulkner, L. R. *Electrochemical Methods*, Wiley: New York, 2001; p 506.

(36) Wong, K.-T.; Chao, T.-C.; Chi, L.-C.; Chu, Y.-Y.; Balaiah, A.; Chiu, S.-F.; Liu, Y.-H.; Wang, Y. *Org. Lett.* **2006**, *8*, 5033.

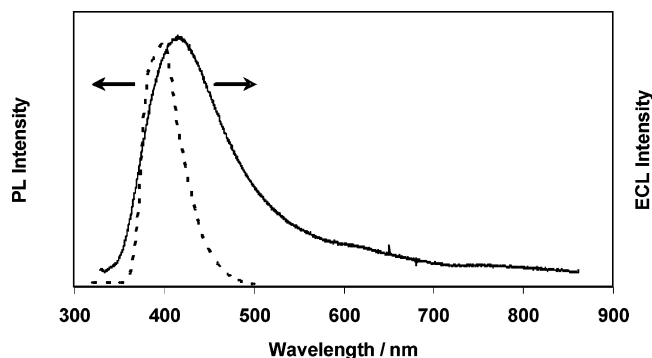
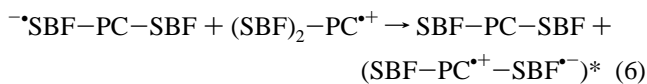
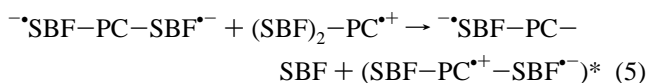


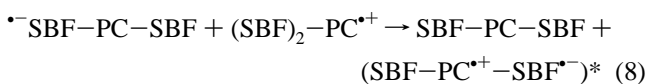
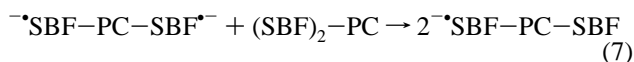
**Figure 6.** Fluorescence spectra (0.53  $\mu\text{M}$ ) of DSBFNPC in 1:1 PhH/MeCN (dotted line) and ECL spectra (solid line) of 0.5 mM DSBFNPC in 0.1 M TBAPF<sub>6</sub> in 1:1 PhH/MeCN with pulsing (0.020 s) between +1.25 and -2.63 V (vs SCE).

upon reduction. The excited DSBFNPC can therefore be produced via two possible electron-transfer mechanisms:

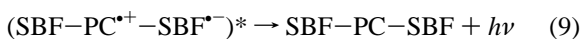
Mechanism I:



Mechanism II:



Both followed by:



The excited state is written in the form suggesting an intramolecular charge-transfer state. These reactions are analogous to the light-emitting reactions of Ru(bpy)<sub>3</sub><sup>2+</sup> given in eqs 1 and 4 of the Introduction. Additional ECL measurements taken as a function of time showed a significant drop in emission intensity that correlated with the cyclic voltammetry that became irreversible upon film formation.

As shown in Figure 6, the ECL of DSBFNPC is characterized by a broad emission band between 350 and 750 nm, and the band appears to have a maximum in 420 nm and a small shoulder at about 620 nm. Upon comparison to the fluorescence

spectra, the ECL spectrum is shifted approximately 20 nm to lower energy. This is probably due to self-absorption (an inner filter effect) as a result of the high concentrations of DSBFNPC needed to obtain measurable ECL compared to fluorescence measurements. In addition, the observed ECL emission band shows significant emission in the longer wavelength region compared to the fluorescence spectrum. This emission might be due to the formation of side products generated during the annihilation.

## Conclusions

We report here electrochemistry and luminescence of a novel ECL emitting compound containing two spirobifluorene groups covalently attached to the *N*-phenylcarbazole group. Semiempirical MNDO calculations of this compound determined that the spirobifluorene is twisted 64° relative to *N*-phenylcarbazole and indicated a weak orbital overlap between these two groups. As a result of this slight interaction between these two groups, the two oxidation waves of the NPC moiety occurred in two separated one-electron oxidation waves. This molecular geometry, however, favors localization of the negative charges on the individual spirobifluorene groups and of the positive charge of the radical cation onto *N*-phenylcarbazole. More importantly, the energy of this annihilation reaction is sufficient enough to generate the singlet excited state and corresponding ECL emission of DSBFNPC. Donor-acceptor architectures such as this may provide a general approach to design new materials exhibiting efficient ECL.

**Acknowledgment.** We thank Mr. Matthew Sartin, Dr. Mario A. Alpuche-Aviles, and Mr. Abolfazl Kiani for technical assistance and helpful discussions and the National Science Foundation, BioVeris, Inc., and the National Science Council of Taiwan for the support of this work.

**Supporting Information Available:** Text giving additional characterization information on DSBFNPC, the UV-vis spectrum of DSBFNPC in various concentrations, and plot of absorbance vs concentration, anodic and cathodic voltammograms of a 1 mM solution of DSBFNPCB in 0.1 TBAPF<sub>6</sub> in 1:1 PhH/MeCN at a platinum electrode (area = 0.031 cm<sup>2</sup>) in various scan rates, and cyclic voltammograms of a 0.5 mM solution of DSBFNPCB in 0.1 TBAPF<sub>6</sub> in 1:1 PhH/MeCN at a platinum electrode (area = 0.002 cm<sup>2</sup>) (scan rate = 0.5 V/s) over various potential windows vs Ag wire QRE, and experimental and simulated voltammograms of a 1 mM of DSBFNPCB at scan rates of 1 and 10 V/s. This material is available free of charge via the Internet at <http://pubs.acs.org>.

JA076033X